The Astrophysical Journal, 663: L109–L112, 2007 July 10

SOLAR FLARE ELECTRON SPECTRA AT THE SUN AND NEAR THE EARTH

Säm Krucker,[1] E. P. Kontar,[2] S. Christe,[1,3] and R. P. Lin[1,3]
Received 2006 September 25; accepted 2007 May 2; published 2007 June 27

ABSTRACT

We compare hard X-ray (HXR) photon spectra observed by the *RHESSI* with the spectra of the electrons in the associated solar impulsive particle events observed near 1 AU by the *WIND* 3D Plasma and Energetic Particle (3DP) instrument. For prompt events, where the inferred injection time at the Sun coincides with the HXR burst, the HXR photon power-law spectral index γ and the in situ observed electron spectral index δ measured above 50 keV show a good linear fit, $\delta = \gamma + 0.1(\pm 0.1)$, with correlation coefficient of 0.83, while for delayed events (inferred injection >10 minutes after the HXR burst) only a weak correlation with a coefficient of 0.43 is seen. The observed relationship for prompt events is inconsistent, however, with both the thin target case, where the escaping electrons come from the X-ray-producing electron population, and the thick target case where some of the accelerated source population escapes to 1 AU and the rest produce the HXRs while losing all their energy to collisions. Furthermore, the derived total number of escaping electrons correlates with the number of electrons required to produce observed X-ray flux but is only about ~0.2% of the number of HXR-producing electrons.

Subject headings: Sun: flares — Sun: particle emission — Sun: X-rays, gamma rays

1. INTRODUCTION

Hard X-ray (HXR) bursts are commonly observed in solar flares, even in microflares that occur as often as every few minutes near solar maximum (Lin et al. 1984, 2001; Krucker et al. 2002). HXR imaging observations show the emission comes mostly from footpoints of flare loops, indicating that the parent energetic electrons rapidly lose their energy to Coulomb collisions in the high-density chromosphere—the thick target case (Brown 1971). In situ observations in the interplanetary medium near 1 AU show that solar impulsive ~1–100 keV electron events occur $\sim 10^3$ times per year near solar maximum over the whole Sun (see Lin 1985). In these events the electron fluxes generally exhibit a rapid onset, with the fastest electrons arriving earliest. Assuming all electrons are released simultaneously from the Sun and travel the same path length, the release time and the path length can be inferred. Some events are prompt, i.e., the inferred release time coincides with the flare HXR burst and/or the solar type III radio burst (Fig. 1); but most events are delayed, i.e., the ≥20 keV electrons appear to be injected from 10 up to 30 minutes later (Krucker et al. 1999; Haggerty & Roelof 2002,\; Maia & Pick 2004; Klein et al. 2005). Recently, however, analysis of three impulsive electron events where the propagation in the interplanetary medium was nearly scatter-free showed that there were two distinct injections, one of low-energy (<15 keV) electrons that started close to the type III radio burst onset at the Sun, and a second injection of high-energy (>15 keV) electrons that was delayed by ~10 minutes (Wang et al. 2006). Presently, it is not understood where and how electrons observed at 1 AU are accelerated at the Sun, nor how they escape into interplanetary space.

Averaged over all events, the power-law indices of electron fluxes $F(E) \sim E^{-\delta}$ above ~50 keV are 3.3 ± 0.7 for in situ observed electron (P. Oakley et al. 2007, in preparation). If electrons with this spectrum lose all their energy through collision (thick target model), they would produce a HXR spectrum $I(\epsilon) \sim \epsilon^{-\gamma}$ with an average power-law index of 2.3 ± 0.7. Such flat HXR spectra are only rarely observed in solar flares. However, this statistical comparison does not discriminate between prompt and delayed impulsive electrons events. Here we survey impulsive events seen in X-ray, radio, and in situ electron observations (Fig. 1) and compare the HXR photon spectra measured by *RHESSI* (Lin et al. 2002) with the in situ observed electron spectra measured by the 3D Plasma and Energetic Particle (3DP) instrument (Lin et al. 1995) on board the *WIND* spacecraft. The comparisons are done only at energies above 50 keV to minimize transport effects (see § 2 for details) and eliminate contamination from flare thermal X-rays. The combination of these two data sets enables, for the first time, the systematic analysis of many events with good spectral resolution for both HXRs and electrons.

2. OBSERVATIONS AND DATA ANALYSIS

From 2002 February (start of *RHESSI* observations) to 2005 December, 132 in situ impulsive electron events were detected by *WIND* above 50 keV with simultaneous *RHESSI* X-ray observations. About 57% of the events have nonthermal HXR emission, ~32% have mostly thermal X-ray emission, and ~12% have no clear X-ray enhancement.

To minimize propagation effects, we select only impulsive electron events that show a clear scatter-free velocity dispersion (with higher energy electrons arriving earlier than electrons at lower energy) consistent with a simple ballistic transport for the first arriving electrons (e.g., Lin 1985). The onsets at different energies are fit to $L = v(t - t_0)$, to obtain both the path length, L, and the solar release time, t_0, where v is the electron velocity (e.g., Krucker et al. 1999). Furthermore, we only select events where the ≥50 keV solar HXR sources seen by *RHESSI* are on the visible solar disk. Those events that coincide within the uncertainties to the time of the X-ray burst, are defined as prompt events.

The 16 prompt events (Table 1) found correspond to magnetically well-connected flares (on average around W44 ± 24), have rather short soft X-ray flare duration (10.2 ± 2.5 minutes), and show at least moderate He^3 enrichments (four of 16 with He^3/He^4 above 0.1; all but one have $He^3/He^4 > 0.01$; G. Mason 2006, private communication). The selected events are therefore a subset of impulsive He^3-rich solar energetic particle events as defined in the classic two-population paradigm of solar energetic

[1] Space Sciences Laboratory, University of California, Berkeley, CA 94720-7450.
[2] Department of Physics and Astronomy, University of Glasgow, Glasgow G12 8QQ, UK.
[3] Department of Physics, University of California, Berkeley, CA 94720-7300.

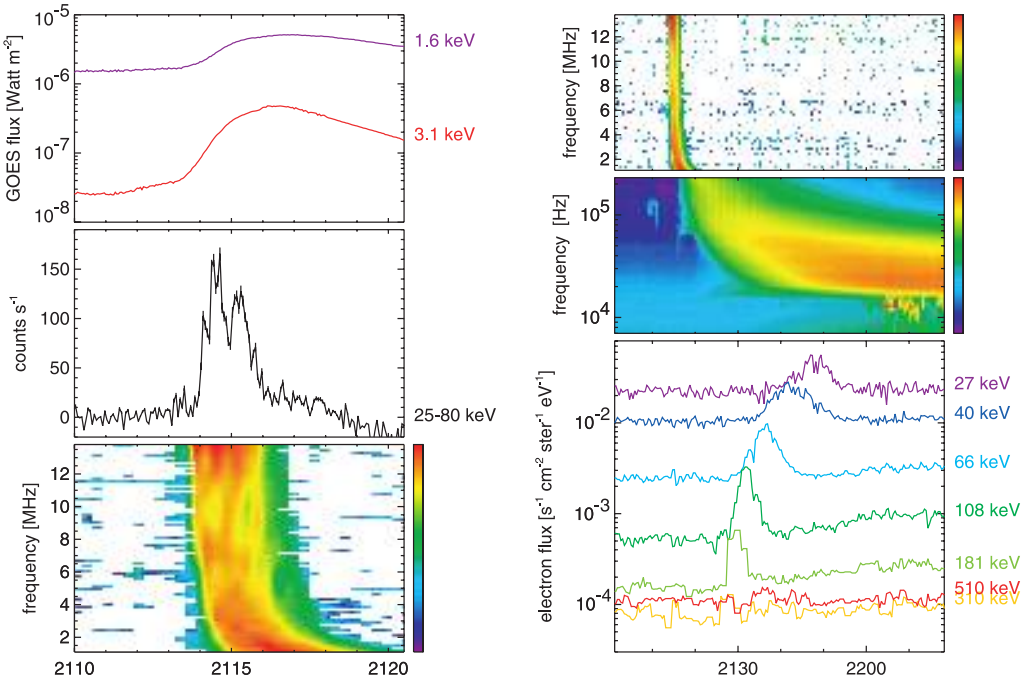

FIG. 1.—Impulsive electron event observed on 2002 October 19: *Left*: From top to bottom, *GOES* soft X-ray light curves, *RHESSI* 25-80 keV light curve, and *WIND*/WAVES radio spectrogram in the 1–14 MHz range are shown (Bougeret et al. 1995). *Right*: An expanded view of the *WIND*/WAVES data including low-frequency observations is presented in the top two panels, while the bottom panel shows in situ observed energetic electrons from 30 to 500 keV detected by *WIND*/3DP. This event (like all events selected in this survey) shows a close temporal correlation between nonthermal HXR emission, radio type III emission in interplanetary space, and in situ observed electrons.

particle events (e.g., Reames 1999). For comparison, 15 events with clear delays (>8 minutes) are analyzed as well. These events are also well connected (W37 ± 27) but are generally related to longer duration flares (40 ± 18 minutes) and show no or low He^3 enrichments (11 of 15 without a significant increase, and four events with He^3/He^4 below 0.03). *RHESSI* imaging shows that the HXR emission in all the selected flares come from footpoints, as most often seen during solar flares, indicating that the accelerated electrons lose their energy by collision in the chromosphere, i.e., thick target emission (Brown 1971).

The in situ observed electron spectra are determined in two ways:

1. Peak flux spectrum.—Constructed by taking the peak flux in each energy channel (due to velocity dispersion, the times of peak are later for lower energies). This would be representative of the injection spectrum if the scattering in the interplanetary medium has the same spatial dependence for all electron energies (the intensity of the scattering can vary with energy, see Lin 1974).
2. Fluence spectrum.—Constructed by integrating over the duration of the event.

TABLE 1

SPECTRAL PARAMETERS OF TEMPORALLY CORRELATED EVENTS SEEN ABOVE 50 keV

HXR Peak Time	*GOES* Class	Flare Location (deg)	γ	δ
2002 Feb 20, 11:06:20	C7.5	N15, W77	$3.8^{-0.1}_{+0.2}$	3.8 ± 0.5
2002 Apr 14, 22:25:37	C7.2	N18, W74	$3.4^{-0.1}_{+0.3}$	3.9 ± 0.2
2002 Apr 25, 05:56:06	C2.5	S19, W08	$2.7^{-0.1}_{+0.4}$	3.3 ± 0.5
2002 Aug 19, 21:01:36	M3.1	S11, W33	$3.2^{-0.1}_{+0.4}$	3.7 ± 0.2
2002 Aug 20, 01:34:24	M5.0	S11, W35	$3.2^{-0.1}_{+0.3}$	3.6 ± 0.5
2002 Aug 20, 08:25:22	M3.4	S07, W40	$2.6^{-0.2}_{+0.3}$	2.5 ± 0.2
2002 Aug 21, 01:38:18	M1.4	S11, W47	$3.5^{-0.1}_{+0.2}$	3.1 ± 0.3
2002 Oct 19, 21:14:30	C5.0	S13, W48	$4.2^{-0.1}_{+0.2}$	3.9 ± 0.5
2003 Sep 30, 08:49:21	C3.2	N09, W45	$3.8^{-0.1}_{+0.3}$	3.7 ± 0.3
2003 Dec 31, 18:22:22	M1.0	N10, W84	$3.6^{-0.1}_{+0.2}$	3.8 ± 0.1
2004 Mar 31, 20:05:37	C7.4	N15, W11	$3.6^{-0.1}_{+0.4}$	3.5 ± 0.3
2004 Oct 30, 03:30:00	M3.3	N13, W20	$3.7^{-0.2}_{+0.4}$	3.3 ± 0.2
2004 Oct 30, 16:32:36	M5.9	N13, W28	$2.8^{-0.2}_{+0.4}$	3.2 ± 0.3
2004 Nov 01, 03:19:08	M1.1	N12, W49	$4.4^{-0.1}_{+0.3}$	4.2 ± 0.2
2005 May 16, 02:40:17	M1.4	S16, E18	$4.1^{-0.1}_{+0.2}$	4.4 ± 0.9
2005 Nov 24, 16:08:35	B1.6	S08, W82	$2.5^{-0.1}_{+0.2}$	2.8 ± 0.3

For all events the peak flux spectrum can be relatively easily determined, while the integration over the duration of the event is not always possible because of spatial changes or the occurrence of a second event. Generally, the shape of the two spectra are similar (see also Lin et al. 1982), with the fitted power-law indices agreeing within 0.2. The derived in situ electron spectra show generally a break around 50 keV (Fig. 2), with a flatter spectrum at lower energy, consistent with previous statistical studies (P. Oakley et al. 2007, in preparation). The resulting uncertainties are typically ~0.3 in the power-law index.

The HXR photon spectra are fitted with a thermal model plus a broken power-law over the duration of the HXR peak that is coincident with the type III radio burst (integration time is ~30–60 s; see, e.g., Fig. 1), using standard *RHESSI* software with pile-up correction (Smith et al. 2002). Above the thermal fit (generally above 30 keV), a broken power law well represents the data with uncertainties from counting statistics below ±0.1 in the power-law index. A correction for X-ray Compton backscattering in the photosphere (albedo correction) for isotropic electrons is applied (Kontar et al. 2006). This correction is generally smaller at higher energies and for flares far away from solar center, and for the events analyzed here, on the average, it steepens the spectral index by 0.14, with extreme values of 0.3. Since most solar flares show the flattest spectra during the peak, with softer spectra during the rise and decay

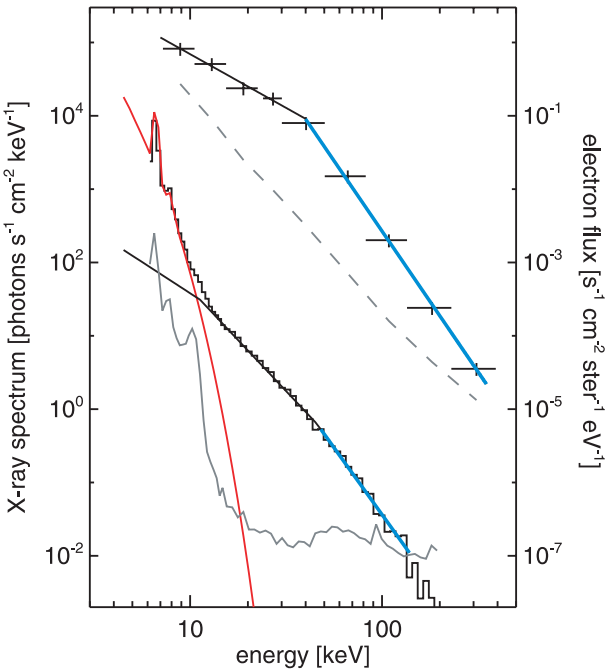

FIG. 2.—Spectra for the event of 2002 April 14. The top curve shows the in situ observed electron peak flux spectrum with the pre-event background spectrum subtracted. A broken power-law fit to the data is shown with spectral indices of −1.5 and −3.9, respectively, and a break around 40 keV. The gray line gives the pre-event background spectrum. Below, the X-ray photon spectrum during the peak of the HXR event is shown in histogram style. A thermal (*red*) and a triple power law are fitted to the data. The thermal fit ($T \sim 14$ MK, EM $\sim 2 \times 10^{48}$ cm^{-3}) dominates below 12 keV, while at higher energies the spectrum is well represented by a broken power law with a break around ~48 keV with spectral indices of 2.8 and 3.4, respectively. The gray curve gives the pre-event and instrumental background. The energy range used in the spectral comparison (Fig. 3) are marked in blue.

(so-called soft-hard-soft effect; e.g., Grigis & Benz 2004), the choice of shorter or longer time interval around the peak gives slightly harder or softer spectra. In extreme cases, this can change the power-law index by ~0.2. Table 1 gives the upper and lower limits to the photon spectral index, not standard deviations, since the above discussed systematic uncertainties dominate over counting statistics.

The break in the photon spectra is around 50 keV (sometimes up to 100 keV), similar to the break observed for the in situ observed electron spectra, but the latter break is much more pronounced with average changes in the power-law index of ~2.0 (P. Oakley et al. 2007, in preparation) compared to ~0.6 for the photon spectra (Conway et al. 2003). The origin of the break is unclear, but it could be a feature of the acceleration mechanism, or possibly a transport effect for the HXR-producing electrons, associated with nonuniform ionization (Kontar et al. 2002) or return current (Zharkova & Gordovskyy 2005). Since those effects tend to affect more the spectrum at lower energies, the observed spectra above the break are the best candidates for a spectral comparison.

Figure 3 (*top*) plots the hard X-ray photon spectral indices versus the in situ observed electron spectral indices for prompt events. A good correlation is seen with flatter HXR flare spectra corresponding to flatter electron spectra. Assuming a relationship of the form $\delta = \gamma + a$, the best fit gives $a = 0.1 \pm 0.1$, with all of the points lying within $a = -0.4$ and $a = +0.5$. For a linear fit, the best fit provides $\delta = (0.8 \pm 0.1)\gamma + (0.9 \pm 0.4)$ with a correlation coefficient of 0.83. This rela-

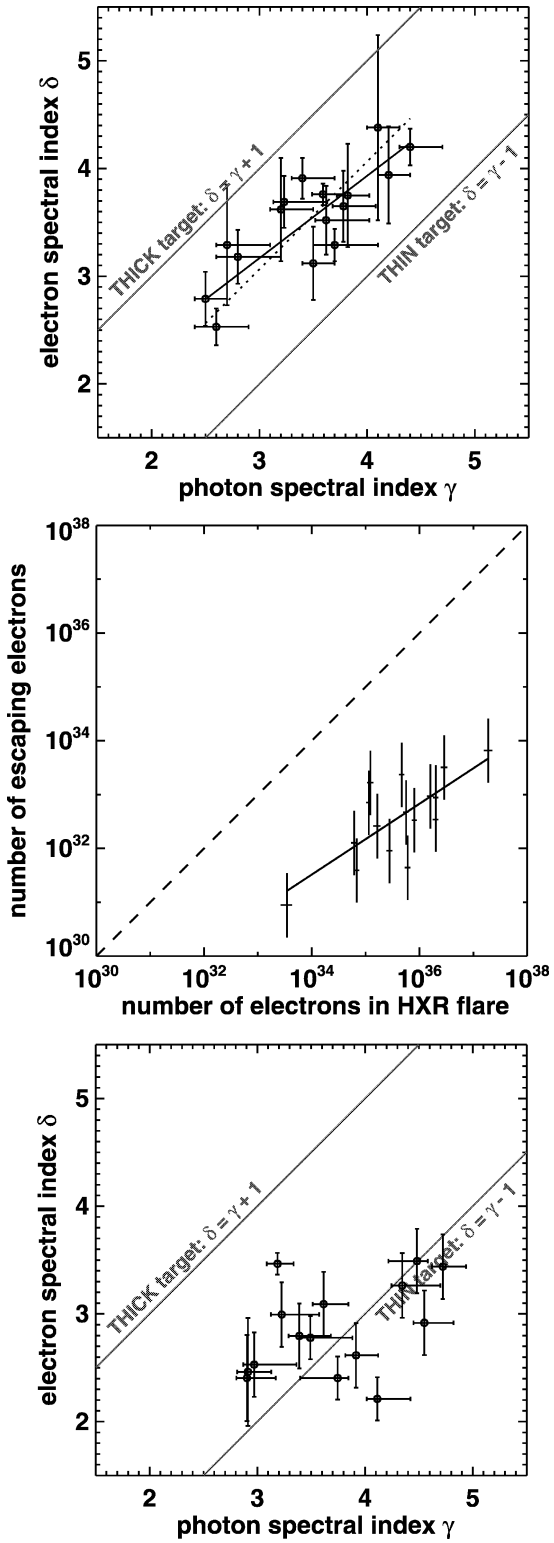

FIG. 3.—*Top*: Correlation plot of the photon spectral index γ and electron spectral index δ for prompt events. A positive correlation with a coefficient of 0.83 is observed. However, neither the thick target nor the thin target model are matched. The solid line is a linear fit to the data, the dotted line is a fit to $\delta = \gamma + a$ giving $a = 0.1 \pm 0.1$. *Middle*: The number of electrons above 50 keV escaping into interplanetary space compared to the number of electrons above 50 keV seen in HXR flares for prompt events. A positive correlation with a coefficient of 0.74 exists, but the number of escaping electrons is more than 2 orders of magnitude smaller. The solid line indicates a power-law fit to the data, $N_{\rm hxr} \propto N_{\rm esc}^{0.7 \pm 0.2}$. *Bottom*: The same as the top figure but for delayed events. No correlation between the power-law indices is observed, suggesting that two different acceleration mechanisms release the HXR-producing electrons and the escaping electron population for delayed events.

tionship is inconsistent with both the thick and the thin target models but consistent with the single event ($\gamma \sim 4.6$ and $\delta \sim 4.0$) studied by Pan et al. (1984). Daibog et al. (1981), however, found ($\gamma \sim 3.7$ and $\delta \sim 2.5$) in their event, consistent with the thin target model. For comparison, Figure 3 (*bottom*) shows the plot of hard X-ray photon spectral indices versus in situ observed electron spectral indices for delayed events, showing only a very weak correlation with a larger scatter. A linear fit provides $\delta = (0.3 \pm 0.2)\gamma + (1.8 \pm 0.6)$ with a correlation coefficient of 0.43.

The total number of energetic electrons needed to produce the observed HXR emission can be computed assuming thick target emission (thin target models require 10^3–10^4 times more electrons to explain the same HXR flux; e.g., Tandberg-Hanssen & Emslie 1988, p. 113) and compared to the number escaping to interplanetary space (Lin 1974). The number of electrons in the interplanetary space depends on the angular extent of the electron events, which is not known for the selected events. We assume a cone of 30° average angular extent, based on statistical studies (e.g., Lin 1974; Reames 1999) and uncertainties calculated using cones of 15° and 60°. Figure 3 (*middle*) plots the number of escaping electrons versus the number of HXR-producing electrons in prompt events. Despite the large error bars, a correlation (correlation coefficient of 0.74) can be seen with large flare events associated with more electrons in interplanetary space. Consistent with earlier findings (Lin 1974; Pan et al. 1984), the number of escaping electrons is on average only ~0.2% of HXR-producing electrons above 50 keV.

3. SUMMARY

Our systematic comparisons of timing, spectra, and number of >50 keV electrons escaping to the interplanetary medium to those electrons producing the HXR burst in the related solar flare show that for prompt events, there is a clear systematic correlation of both the power-law spectral indices and of the total number of electrons. This is consistent with a single process accelerating both the escaping and HXR-producing electrons. Only a very weak correlation of the spectral indices is found for delayed events suggesting that in those events the acceleration of HXR-producing electrons is not as closely related to that producing the escaping electrons as for prompt events. For the prompt events, however, the observed relationship of the power-law indices of the HXR photon spectra to that of the escaping electrons is not consistent with the simplest thick target picture—that of a single acceleration occurring in the corona, with a few electrons escaping directly into interplanetary space and the rest going down to the chromosphere and losing all their energy to collisions while producing the HXRs. We suggest the possibility that a small number of electrons are accelerated in the initial magnetic reconnection between oppositely directed field lines in the interchange reconnection model (e.g., Heyvaerts et al. 1977), with the upward-moving ones escaping to interplanetary space while the downward-moving electrons are trapped on stretched closed field lines. As those field lines shrink, the trapped electrons are further accelerated, thus modifying their spectrum and increasing the number of electrons above 50 keV (e.g., Karlicky & Kosugi 2004), and these electrons then produce the hard X-rays through thick target emission. Detailed modeling is needed to test this hypothesis.

The work was supported through NASA contract NAS 5-98033 for *RHESSI* and grant NNG 05GH18G for *WIND*. E. P. K. gratefully acknowledges the support of a PPARC Advanced Fellowship.

REFERENCES

Brown, J. C. 1971, Sol. Phys., 18, 489
Bougeret, J.-L., et al. 1995, Space Sci. Rev., 71, 231
Conway, A. J., Brown, J. C., Eves, B. A. C., & Kontar, E. 2003, A&A, 407, 725
Daibog, E. I., et al. 1981, Adv. Space Res., 3, 73
Grigis, P. C., & Benz, A. O. 2004, A&A, 426, 1093
Haggerty, D. K., & Roelof, E. C. 2002, ApJ, 579, 841
Heyvaerts, J., Priest, E. R., & Rust, D. M. 1977, ApJ, 216, 123
Karlický, M., & Kosugi, T. 2004, A&A, 419, 1159
Kontar, E. P., Brown, J. C., & McArthur, G. K. 2002, Sol. Phys., 210, 419
Kontar, E. P., MacKinnon, A. L., Schwartz, R. A., & Brown, J. C. 2006, A&A, 446, 1157
Klein, K.-L., Krucker, S., Trottet, G., & Hoang, S. 2005, A&A, 431, 1047
Krucker, S., Christe, S., Lin, R. P., Hurford, G. J., & Schwartz, R. A. 2002, Sol. Phys., 210, 445
Krucker, S., Larson, D. E., & Lin, R. P., & Thompson, B. J. 1999, ApJ, 519, 864
Lin, R. P. 1974, Space Sci. Rev., 16, 189
———. 1985, Sol. Phys., 100, 537
Lin, R. P., Feffer, P. T., & Schwartz, R. A. 2001, ApJ, 557, L125
Lin, R. P., Mewaldt, R. A., & van Hollebeke, M. A. I. 1982, ApJ, 253, 949
Lin, R. P., Schwartz, R. A., Kane, S. R., Pelling, R. M., & Hurley, K. C. 1984, ApJ, 283, 421
Lin, R. P., et al. 1995, Space Sci. Rev., 71, 125
———. 2002, Sol. Phys., 210, 3
Maia, D. J. F., & Pick, M. 2004, ApJ, 609, 1082
Pan, L.-D., Lin, R. P., & Kane, S. R. 1984, Sol. Phys., 91, 345
Reames, D. V. 1999, Space Sci. Rev., 90, 413
Smith, D. M., et al. 2002, Sol. Phys., 210, 33
Tandberg-Hanssen, E., & Emslie, A. G. 1988, The Physics of Solar Flares (Cambridge: Cambridge Univ. Press)
Wang, L., Lin, R. P., Krucker, S., & Gosling, J. T. 2006, Geophys. Res. Lett., 33, 3106
Zharkova, V. V., & Gordovskyy, M. 2005, A&A, 432, 1033